

Transition Metal Dopants with Unusual Ligands

M. T. Olm, R. S. Eachus, W. G. McDugle, and R. C. Baetzold
Imaging Materials and Media, Research & Development
Eastman Kodak Company
Rochester, NY 14650, USA

Abstract

Transition metal (TM) dopant complexes are used to control the photographic features of many types of silver halide emulsions. This paper reviews recent trends in TM dopant technology. The concept of “doping” has evolved from a simple picture in which a metal ion replaces Ag^+ to one where a hexa-coordinated anionic complex, $(\text{MX}'_6)^{m-}$ or $(\text{MX}'_{6-n}\text{L}_n)^{m-}$, replaces the lattice unit, $(\text{AgX}_6)^{5-}$. Recently, we have shown that complicated organic ligands can be incorporated into the silver halide lattice as part of a transition metal complex.¹⁻³ Such large ligands are accommodated by the replacement of higher $(\text{Ag}_n\text{X}_m)^{p-}$ clusters. An example would be $\text{IrCl}_5(\text{N-methyl pyrazine})^{1-}$, a dopant extensively studied in the silver halide lattice by electron magnetic resonance and computational methods.^{2,3}

Introduction

A combination of fundamental spectroscopic studies and advanced computations of structure and energy has facilitated the development of new dopant technologies for commercial photographic materials. We begin with a brief historical review of this important technology and then lead into a discussion of recent experiments performed on state-of-the-art dopant materials.

A dopant is defined as an ion or complex that is incorporated in a dispersed manner into the silver halide lattice. This differentiates it from material occluded as a separate phase, or adsorbed onto the AgX surface. In the simplest example, a foreign ion replaces a lattice anion or cation, e.g., the substitution of Br^- by I^- or Ag^+ by Ir^{3+} . In the case of Ir^{3+} , the point ion model is supported by electron magnetic resonance (EMR) data obtained from doped single crystals grown at high temperatures, and is consistent with conductivity measurements made on these types of samples. In emulsion grains, however, the behavior of Ir^{3+} (and other TM ions) are more completely understood if we consider the dopant to be a hexa-coordinated anionic complex, i.e., $(\text{IrX}_6)^{3-}$ where $\text{X} =$ the lattice anion.⁴

Recognizing the importance of the ligand shell led to the development of practical silver halide doping technologies that included anionic complexes with non-lattice halide ions. Thus, $(\text{MX}'_6)^{3-}$ complexes were doped into AgX' , where $\text{X} = \text{F}^-, \text{Cl}^-, \text{Br}^-, \text{I}^-$ or combinations of these anions, and $\text{X}' = \text{Cl}^-, \text{Br}^-, \text{I}^-$ or their mixtures. Furthermore, it

was discovered that complexes with non-halide ligands, i.e., $(\text{MX}'_{6-n}\text{L}_n)^{m-}$, can also be incorporated substitutionally into the silver halide lattice during precipitation.^{5,6} The earliest examples were, most probably, inadvertent, such as the solution decomposition products $[\text{IrCl}_5(\text{H}_2\text{O})]^{3-}$ and $[\text{RhCl}_5(\text{H}_2\text{O})]^{3-}$.^{5,6}

Subsequent studies of dopants included complexes with pseudo-halides and mixed coordination shells of halides and pseudo-halides. The principle pseudohalide example was cyanide,^{7,8} but other anionic groups known to mimic the properties of halides include CN^- , OCN^- , SCN^- , SeCN^- , TeCN^- , N_3^- , $\text{C}(\text{CN})_3^-$ and CH^- . Examples of L were further expanded to include small ligands other than H_2O , such as NO^+ , NS^+ , O_2 , and CO .⁹⁻¹¹ With just these components, a multitude of new dopant complexes were possible. By way of illustration, reference 9 describes examples of the form $[\text{M}(\text{NO})\text{L}_5]^{m-}$, where $m = -1, -2$, or -3 . Here $\text{L} = \text{F}^-, \text{Cl}^-, \text{Br}^-$ or I^- , a combination of these halides, CN^- , a combination of halides and CN^- , or a combination of halides, cyanide, and up to two aquo ligands!

Electron magnetic resonance (EMR) studies of representative examples of these more complicated dopant complexes, such as $\text{Fe}(\text{CN})_6^{4-}$ and $[\text{MCl}_5(\text{NO})]^{3-}$, verified that they could be incorporated into the silver halide lattice intact. EMR methods were also used to probe interactions of these complexes with photogenerated electrons and holes, and it was possible to relate their trapping properties to the emulsion's enhanced photographic features. Advanced structural computations showed that stable structures result when these dopants replace $(\text{AgX}_6)^{5-}$ lattice fragments.¹³⁻¹⁶

An early example of a dopant that must replace a lattice unit larger than $(\text{AgX}_6)^{5-}$ resulted from an evaluation of oligomeric complexes. The prototypic example was $(\text{Ir}_2\text{Cl}_{10})^{4-}$ which, calculations suggest, replaces $(\text{Ag}_2\text{X}_{10})^{8-}$ in AgBr or AgCl .¹² Cyclic oligomeric units as large as $\text{M}_{10}\text{L}_{38}$ were studied. This technology provided a unique way of introducing metal dopant ions at adjacent sites in the silver halide lattice.¹²

Recently, we have shown that TM complexes with bulky organic ligands can also be incorporated substitutionally into AgX .^{1,2} To accommodate the substantial lattice mismatch that occurs in these cases, it is frequently necessary for the dopant to replace $(\text{Ag}_n\text{X}_m)^{p-}$ clusters. A prime example is $\text{IrCl}_5(\text{N-methyl pyrazine})^{1-}$. This complex has been studied extensively in AgCl emulsions by electron magnetic resonance and computational methods.^{2,3}

The possibility that bulky complexes could be incorporated into the AgX lattice during precipitation opened up many new avenues for dopant design. Table 1 gives a few representative examples.

Table 1: Examples of dopant complexes with organic ligands, taken from reference 1.

$\text{Na}_3[\text{Fe}(\text{CN})_5\text{L}]$	
Where L =	3,8 phenanthroline
Pyrazine	1-methyl-4-(4py)pyridinium
4,4' bipyridine	N-Me-pyrazinium
3,3' dimethyl 4,4' bipyridine	4-Cl-pyridine
Potassium pentachloride (pyrazine) ruthenate (II)	
Potassium tetracyano (ethylenediamine) cobaltate (III)	
Potassium pentacyano(thiazole)rhodate (III)	
Potassium tetrachloro bis(dimethylsulfoxide) rhodate (III)	
Potassium pentachloro(pyrazine)iridate (III)	
Potassium tetrachlorobiscis(pyrazine)iridate (III)	
Potassium tetrachlorotrans(pyrazine)iridate (III)	
Potassium trichloro tris(pyrazine) iridate (III)	
Potassium pentachloro(thiazole)iridate (III)	
Potassium tetrachloro(oxalato)iridate (III)	
$\text{K}_5[\text{IrCl}_5(\text{pyz})\text{Ru}(\text{CN})_5]$	
$\text{Na}_6[\text{Fe}(\text{CN})_5(4,4'\text{-bipyridine})(\text{CN})_5\text{Fe}]$	

The purpose of this paper is to review the direct and indirect evidence for the rather surprising incorporation of this class of dopants. We begin by reviewing EMR data that provides indirect evidence for incorporation of representative "organic ligand" dopants derived from $\text{Fe}(\text{CN})_6^{4-}$ and IrCl_6^{3-} . The parent compounds are widely used in photographic emulsions, and they have been the subject of extensive mechanistic studies. They represent a variety of carrier-trapping behaviors, acting either as amphoteric hole traps/shallow electron traps or as deep electron traps. We end by reviewing recently published studies of $[\text{IrCl}_5(\text{N-methyl pyrazine})]^{1-}$, since they provide the strongest evidence for dopant incorporation intact. We will touch very briefly on some of the trapping properties imparted by the organic ligand and mention some of the photographic benefits these dopants can provide.

Summary of Experimental Conditions

All of the EMR data summarized below were obtained from cubic silver chloride microcrystals prepared as dispersions in aqueous gelatin by standard double-jet precipitation techniques. Further details on microcrystal size and precipitation conditions are given in references 1 and 2. For EMR studies, the amount of gelatin peptizer present in each sample was minimized by three aqueous dilution and centrifugation treatments. The resultant powders were dried in air following an acetone wash, and then stored at 4 °C.

Details of the electron paramagnetic resonance (EPR) experiments, performed at both X-band and Q-band frequencies, and electron nuclear double resonance (ENDOR) experiments performed at X-band frequency, are given in references 1 and 2. Generally, spectra were obtained at temperatures between 8 and 20 K, after the sample had been exposed to band gap light at temperatures between 180 and 300 K.

Details of the structure and energy level calculations are given in reference 2.

Details of dopant synthesis are given in reference 1 and the references contained therein, and in reference 2. Dopant complexes were characterized by NMR, UV-Vis and IR spectroscopies.

Details of photographic testing are described in reference 1.

Review of EMR Studies of Dopants Derived from the $\text{Fe}(\text{CN})_6^{4-}$ Parent Complex

We first consider AgCl cubic emulsion grains doped with $[\text{Fe}(\text{CN})_5(4,4'\text{-bipyridine})]^{3-}$. No EPR signals were observed from the doped grains as prepared. After their exposure to 365 nm light between 260 K and room temperature, EPR signals were observed at 5 - 8 K. These signals were not observed from undoped control samples after light exposure. The same EPR signals were observed after the doped, unexposed silver chloride emulsion was placed in an oxidizing atmosphere of chlorine gas. Discernible in these signals were powder pattern lineshapes like those typically observed from a randomly oriented ensemble of low symmetry paramagnetic species in a powder or frozen solution. These powder patterns were assigned to four distinct Fe species, each with a low-spin d^5 electronic configuration. The g-factors derived for each species are given in Table 2. Consistent with their assignment to low-spin d^5 complexes, the signals were fairly narrow; typically, the lines at g_1 had linewidths at half maximum of about 10 mT.

Table 2: EPR parameters measured for $[\text{Fe}(\text{III})(\text{CN})_5(4,4'\text{-bipyridine})]^{2-}$ centers in AgCl powder. These centers were produced by band-gap exposure at 260 K.

Site	g_1	g_2	g_3
I	2.924	2.286	1.376
II	2.884	2.263	*
III	2.810	2.213	*
IV	*	2.093	*
* feature not resolved			

Because these EPR powder patterns were not detected before light exposure and were produced by an oxidizing atmosphere, the $[\text{Fe}(\text{CN})_5(4,4'\text{-bipyridine})]^{3-}$ complex must be incorporated with the metal ion in the low-spin Fe(II) state (which is "EPR silent"). This dopant must trap a hole to produce an Fe(III) center during exposure to chlorine or light.

By analogy to previous studies of substitutional low-spin d^5 transition metal complexes, in particular, the parent $[\text{Fe}(\text{CN})_6]^{3-}$ in AgCl ,¹³ these complexes likely differ in the arrangement of the associated silver ion vacancies, which are necessary to provide charge neutrality in the silver chloride lattice.

To determine if the dopant was incorporated primarily as $[\text{Fe}(\text{CN})_5(4,4'\text{-bipyridine})]^{3-}$ with the ligands surrounding the ferrous ion intact, we compared the observed EPR spectra with those obtained upon doping silver chloride powders with the most chemically-feasible, ligand-exchanged contaminants of the dopant salt that might be produced during synthesis of the dopant or precipitation of the emulsion. The species $[\text{Fe}(\text{CN})_6]^{3-}$, $[\text{Fe}(\text{CN})_5\text{H}_2\text{O}]^{2-}$, $[\text{Fe}(\text{CN})_5\text{Cl}]^{3-}$, and $[\text{Fe}_2(\text{CN})_{10}]^{6-}$ were investigated. The EPR spectra of these Fe(III) species produced in the silver chloride grains by exposure to light or chlorine were quite dissimilar from those assigned to the four species derived from $[\text{Fe}(\text{CN})_5(4,4'\text{-bipyridine})]^{3-}$.

From the foregoing we conclude that the 4,4'-bipyridyl ligand was sufficiently stable in aqueous solution to minimize its exchange with chloride or water during coprecipitation. Considering (i) the observation of well-resolved EPR powder patterns from the doped emulsion, (ii) the high yields of the low-spin Fe(III) photo-products, and (iii) the propensity of low-spin Fe(III) ions for six-fold coordination, we conclude that the dopant is incorporated substitutionally into silver chloride. Despite the presence of the bulky organic ligand, it is not occluded as a separate phase or adsorbed as a surface species. Calculations suggest that ignoring charge-compensating silver ion vacancies, this dopant substitutes for an $[\text{Ag}_2\text{Cl}_8]^{6-}$ moiety in the lattice.

As has been observed previously for the parent complex $[\text{Fe}(\text{CN})_6]^{3-}$ in AgCl , the $[\text{Fe}(\text{CN})_5(4,4'\text{-bipyridine})]^{3-}$ complexes were amphoteric. Actinic exposures at temperatures below 200 K produced a symmetric EPR line at $g = 1.88$ from electrons shallowly trapped at sites with less than their full complement of silver ion vacancies.¹³⁻¹⁵

Photographic studies of 0.5 μm AgBr octahedral grains found that $[\text{Fe}(\text{CN})_5(4,4'\text{-bipyridine})]^{3-}$ reduced dye desensitization, as expected for dopants acting as shallow electron traps. The onset of this behaviour occurred at a lower dopant concentration with a lower fog level than for the parent $[\text{Fe}(\text{CN})_6]^{4-}$.¹

EPR studies also showed that, after exposure, silver chloride grains doped with the related ligand-bridged compound $[\text{Fe}(\text{CN})_5(4,4'\text{-bipyridine})(\text{CN})_5\text{Fe}]^{6-}$ exhibited unique EPR spectra, with the characteristics of low-spin d^5 complexes. This raises the possibility that this compound could also be incorporated into the grain intact. It certainly introduces both hole traps and shallow electron traps into the emulsion grain.

Emulsions doped with $[\text{Fe}(\text{EDTA})]^-$, or $[\text{Fe}(\text{C}_2\text{O}_4)_3]^{3-}$ showed no EPR signals prior to, or following irradiation or exposure to Cl_2 . Furthermore, elemental analyses by ion coupled plasma-atomic emission spectroscopy (ICP-AES) showed doping with these complexes did not increase the Fe level above background. Generally, it appears that at least

half of the ligand shell must be made up of halide or pseudo halide ligands to ensure good incorporation. In keeping with this observation, the authors in reference 1 report for the dopant series, potassium tetrachloro(oxalate)iridate (III), potassium dichloro(bis-oxalate) iridate (III), and potassium (tris-oxalate) iridate (III), that only the first compound gave any significant photographic effect. (The control compound, potassium oxalate, also had little or no effect.)

Review of EMR Studies of Dopants Derived from the $(\text{IrCl}_6)^{3-}$ Parent Dopant

AgCl cubic emulsions doped with the dopants listed in Table 3 were prepared and studied by EPR. Total Ir incorporation for the $[\text{IrCl}_5\text{thiazole}]^{2-}$, $[\text{IrCl}_5\text{pyrazine}]^{2-}$ and $[\text{IrCl}_5\text{N-methylpyrazine}]^{1-}$ dopants, as measured by ICP-AES, matched that measured for the $(\text{IrCl}_6)^{3-}$ parent dopant.

No EPR signals were observed from any of the samples before light exposure. Exposure to actinic radiation between 180 and 240 K produced powder-pattern spectra with the principle g -factors noted in Table 3.^{1,2} Similar spectra were not produced on chlorination. At sufficiently low temperatures of exposure, we observed strong signals from the intrinsic self-trapped hole center in all of the doped samples.

Table 3: EPR parameters measured for iridium complexes in AgCl . These centers were produced by band-gap exposure between 180 and 240 K.

Ligand, n	g_1	g_2	g_3
Cl , n = 3	2.772	2.772	1.883
H_2O , n = 2	3.006	2.702	<2
thiazole, n = 2	2.911	2.634	1.871
pyrazine, n = 2	3.043	2.503	1.823
N-methyl pyrazinium, n = 1	1.9785	1.9785	1.9510

The spectra from the first two control dopants matched those reported previously for the $(\text{IrCl}_6)^{4-}$ and $(\text{IrCl}_5\text{H}_2\text{O})^{3-}$ d^7 complexes in AgCl . The spectra from these control dopants and those from $[\text{IrCl}_5\text{thiazole}]^{2-}$ and $[\text{IrCl}_5\text{pyrazine}]^{2-}$ exhibited hyperfine splittings from the central iridium ion and superhyperfine splittings from neighboring chloride ions. The magnitudes of the splittings differed from complex to complex. The hyperfine splittings confirm the presence of iridium in the complexes produced by doping with $[\text{IrCl}_5\text{thiazole}]^{2-}$ and $[\text{IrCl}_5\text{pyrazine}]^{2-}$. Noting (i) the unique powder patterns seen for these two dopants, (ii) that these patterns differed from the possible contaminants or decomposition products ($(\text{IrCl}_6)^{3-}$ and $(\text{IrCl}_5\text{H}_2\text{O})^{2-}$), and (iii) the high total Ir incorporation and the good stability of the $[\text{IrCl}_5\text{thiazole}]^{2-}$ and $[\text{IrCl}_5\text{pyrazine}]^{2-}$ dopant solutions, we feel there is strong empirical evidence that both dopants are being incorporated into the AgCl lattice intact. The narrow EPR lines suggest dispersed, substitutional incorporation. They both trap electrons on exposure.

These dopants have trapping properties that are not dramatically different from those of $(\text{IrCl}_6)^{3-}$ and so are useful for improving reciprocity behavior with varying effects on other photographic features.¹

Review of $\text{IrCl}_5(\text{N-methyl pyrazine})^{1-}$ - Doped AgCl Studies

A Q-band EPR spectrum obtained after light exposure of an $[\text{IrCl}_5\text{N-methylpyrazine}]^{1-}$ -doped AgCl emulsion is shown in Fig. 1. It is clear from this figure and Table 3 that this powder pattern is substantially less anisotropic than those obtained from the other Ir^{2+} species described above. (The spectral anisotropy is represented by the spread in the g_1 to g_3 values.) As discussed in references 2 and 3, this is because the photoelectron is primarily trapped onto the positively charged N-methyl pyrazinium ligand, reminiscent of the localization of the trapped electron in NO^+ -derived orbitals for $[\text{Os}(\text{NO})\text{Cl}_5]^{2-}$ and $[\text{Ru}(\text{NO})\text{Cl}_5]^{2-}$ dopants.¹⁶

This narrow, structureless EPR powder pattern is suitable for study by ENDOR spectroscopy. ENDOR (electron nuclear double resonance spectroscopy), is a highly sensitive NMR technique uniquely tagged to the EPR signal of interest. In the solid state, the higher resolution of NMR compared to EPR yields greater details about ions surrounding the paramagnetic center of interest. For this reason, multifrequency EPR spectroscopy and ENDOR spectroscopy were recently combined with advanced computational techniques in a study of $[\text{IrCl}_5\text{N-methylpyrazine}]^{1-}$ in order to obtain an understanding of its structure and trapping properties in AgCl dispersions.

These experiments are covered in detail in references 2 and 3. Summarizing the results, two sites are detected by EPR. The number of associated charge compensating silver ion vacancies differentiates them. For the predominant $[\text{IrCl}_5\text{N-methylpyrazine}]^{1-}$ center with four neighboring vacancies, ENDOR measurements revealed hyperfine splittings from both ring and methyl protons. Assignments of the ENDOR lines were facilitated by doping AgCl grains with $[\text{IrCl}_5\text{N-methylpyrazine}]^{1-}$ complexes in which the organic moiety was enriched with ^{13}C and/or substituted with ^2D .

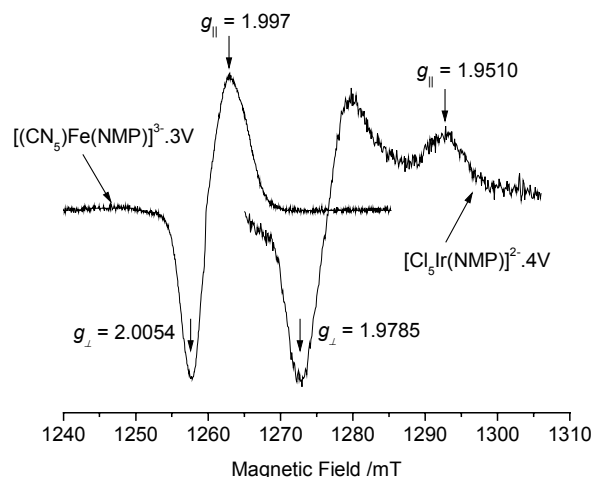


Figure 1. Q-band EPR spectra obtained at 82 K from AgCl dispersions doped with $[(\text{CN})_5\text{Fe}(\text{NMP})]^{2-}$ or $[\text{Cl}_5\text{Ir}(\text{NMP})]^{1-}$. The spectra were obtained following 365 nm irradiation at 85 K and 210 K, respectively.

Theory predicts that a stable lattice can be achieved if $[\text{IrCl}_5\text{N-methylpyrazine}]^{1-}$ substitutes for $(\text{Ag}_2\text{Cl}_7)^{5-}$ with the NMP ring rotated 45° with respect to the equatorial chloride ligands.

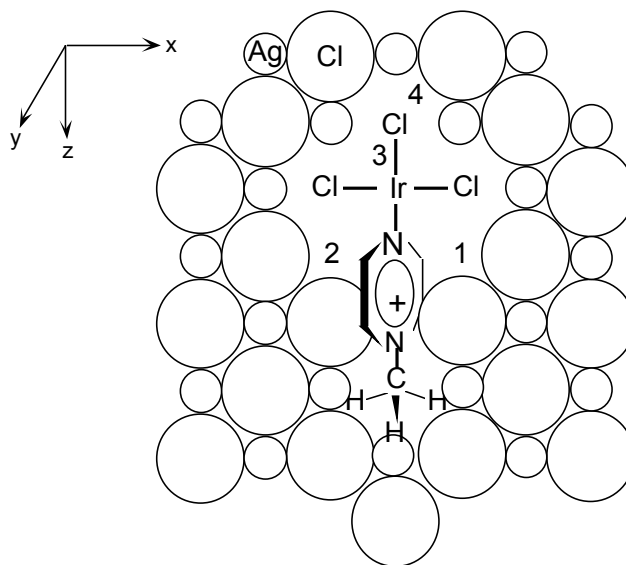


Figure 2. Model calculated for $[\text{Cl}_5\text{Ir}(\text{NMP})]^{1-}$ center with 4 bound vacancies. The dopant substitutes for $(\text{Ag}_2\text{Cl}_7)^{5-}$. The Cl ligands coordinated to Ir above and below the plane are omitted for clarity. Sites for the bound vacancies are marked 1-4, with position 3 above the plane and position 4 below the plane.

Calculations also show that the majority of dopant centers will be fully charge-compensated by association with four silver ion vacancies (Fig. 2). These are retained after electron trapping. The vacancy binding energies are so large that the over-compensated donor produced after trapping ionizes before the extra vacancy diffuses away. Experimental ^1H hyperfine data obtained by powder ENDOR spectroscopy are consistent with the unpaired electron distribution calculated by Hartree-Fock methods for the favored vacancy geometry of $\{[\text{IrCl}_5\text{N-methylpyrazine}]^{1-} \cdot 4\text{V}\}$.

Photo-EPR experiments suggest a small population of under-compensated $\{[\text{IrCl}_5\text{N-methylpyrazine}]^{1-} \cdot 3\text{V}\}$ centers also exist in most of the dispersions studied.

The calculated one-electron energy levels are shown in Fig. 3.

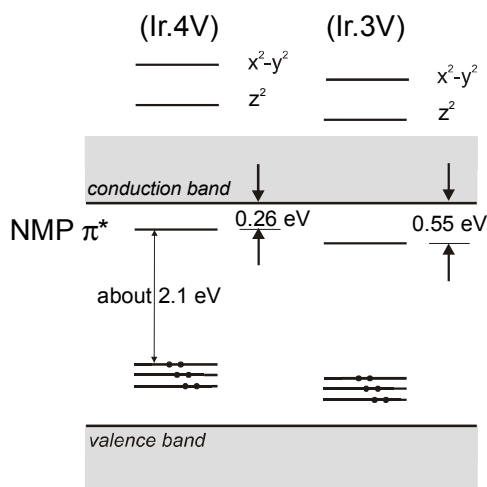


Figure 3. One-electron energy level models calculated for $[\text{Cl}_5\text{Ir}(\text{NMP})]^{1-}$ centers in AgCl with three ($\text{Ir}3\text{V}$) and four ($\text{Ir}4\text{V}$) bound vacancies.

Doping with $[\text{Fe}(\text{CN})_5\text{N-methylpyrazine}]^{2-}$

As part of the studies just described, the $\text{Cl}_5\text{Ir-}$ moiety was replaced by $(\text{CN})_5\text{Fe-}$ and the effects on the donor's magnetic resonance parameters were monitored.³ The shift in the powder pattern shown in Fig. 1 for $[\text{Fe}(\text{CN})_5\text{N-methylpyrazine}]^{2-}$ was presented as evidence that the Ir and Fe metal ions are bound to N-methylpyrazine moieties in the AgCl lattice. A powder ENDOR spectrum obtained from $[\text{Fe}(\text{CN})_5\text{N-methylpyrazine}]^{2-}$ also showed well-resolved proton resonances. It was proposed that the g-factor variations arose from different spin-orbit contributions of the Ir and Fe central ions. The g-shifts also indicate that some spin density resides on the metal ion.

The dopant, $[\text{Fe}(\text{CN})_5\text{N-methylpyrazine}]^{2-}$ like $[\text{IrCl}_5\text{N-methylpyrazine}]^{1-}$, is a very deep electron trap. It is interesting to note that substitution of N-methylpyrazine for CN^- causes a dramatic change in trapping properties from the shallow electron trapping and hole trapping characteristic of the parent compound, $[\text{Fe}(\text{CN})_6]^{4-}$.

Conclusion

The silver halides are capable of incorporating remarkably large dopant complexes substitutionally into the lattice. The examples given here are primarily hexa-coordinated transition metal complexes with a ligand shell comprised of halide, pseudo-halide and/or organic ligands. The possibility of incorporating such complexes into the emulsion grain provides new opportunities for dopant applications and new challenges in understanding. Measurements supporting the assertion that such large moieties can be incorporated intact were presented. The most detailed mechanistic study to date was for $[\text{IrCl}_5\text{N-methylpyrazine}]^{1-}$. EPR, ENDOR, and theoretical tools were used together to provide detailed information about the structure and trapping properties of these complexes.

References

1. U.S. Patent 5,360,712, Myra T. Olm, Woodrow G. McDugle, Sherrill A. Puckett, Traci Y. Kuromoto, Raymond S. Eachus, Eric L. Bell, Robert D. Wilson, Nov. 1, 1994.
2. Raymond S. Eachus, Thomas D. Pawlik, Roger C. Baetzold, Donald A. Crosby, Woodrow G. McDugle *J. Phys.: Condens. Matter* 12, 2535 (2000).
3. Thomas D. Pawlik, Raymond S. Eachus, Roger C. Baetzold, Woodrow G. McDugle, *J. Phys.: Condens. Matter* 12, 2555 (2000).
4. Raymond S. Eachus, Richard R. Graves, *J. Chem. Phys.* 65, 1530 (1976).
5. Raymond S. Eachus, Myra T. Olm, *Nippon Shashin Gakkaishi* 54, 294 (1991).
6. Raymond S. Eachus, Myra T. Olm, *Cryst. Lattice Defects Amorphous Mater.* 18, 297 (1989) and references therein.
7. U.S. Patent 4,945,035, John E. Keevert, Jr., Woodrow G. McDugle, Raymond S. Eachus, July 31, 1990.
8. U.S. Patent 4,937,180, Alfred P. Marchetti, Woodrow G. McDugle, Raymond S. Eachus, June 26, 1990.
9. U.S. Patent 4,933,272: McDugle; Woodrow G., Anthony D. Gingello, John A. Haefner, John E. Keevert, Jr., Alfred P. Marchetti June 12, 1990
10. U.S. Patent 4,981,781, Woodrow G. McDugle, John E. Keevert, Jr., Alfred P. Marchetti, Jan. 1, 1991
11. U.S. Patent 5,037,732, Woodrow G. McDugle, Alfred P. Marchetti, John E. Keevert, Jr., Marian S. Henry, Myra T. Olm, Aug. 6, 1991.
12. U.S. Patent 5,024,931: Francis J. Evans, Ralph W. Jones, Jr., Robert D. Wilson, June 18, 1991.
13. Myra T. Olm, Raymond S. Eachus, *Radiat. Eff. Defects Solids* 135, 101 (1995).
14. Myra T. Olm, Raymond S. Eachus, *Radiat. Eff. Defects Solids* 150, 463 (1999).
15. Martin T. Bennebroek, Jan Schmidt, Raymond S. Eachus, Myra T. Olm, *J. Phys.: Condens. Matter* 9, 3227 (1997).
16. Raymond S. Eachus, Roger C. Baetzold, Thomas D. Pawlik, O. G. Poluektov, Jan Schmidt, *Phys. Rev. B: Condens. Matter Mater. Phys.* 59, 8560 (1999).